



## OPEN Mutated IL-32 $\theta$ (A94V) inhibits COX2, GM-CSF and CYP1A1 through AhR/ARNT and MAPKs/NF- $\kappa$ B/AP-1 in keratinocytes exposed to PM<sub>10</sub>

Jinju Kim<sup>1</sup>, Chae-Min Lim<sup>1</sup>, Nahyun Kim<sup>1</sup>, Hong-Gyum Kim<sup>2</sup>, Jin-Tae Hong<sup>3</sup>, Young Yang<sup>4</sup>✉ & Do-Young Yoon<sup>1</sup>✉

Exposure to particulate matter (PM) in the air harms human health. Most studies on particulate matter's (PM) effects have primarily focused on respiratory and cardiovascular diseases. Recently, IL-32 $\theta$ , one of the IL-32 isoforms, has been demonstrated to modulate cancer development and inflammatory responses. This study revealed that one-point mutated IL-32 $\theta$  (A94V) plays an important role in attenuating skin inflammation. IL-32 $\theta$  (A94V) inhibited PM-induced COX-2, a pro-inflammatory cytokine GM-CSF and CYP1A1 in PM-exposed human keratinocytes HaCaT cells. IL-32 $\theta$  (A94V) modulating effects were mediated via down-regulating ERK/p38/NF- $\kappa$ B/AP-1 and AhR/ARNT signaling pathways. Our study indicates that PM triggers skin inflammation by upregulating COX-2, GM-CSF and CYP1A1 expression. IL-32 $\theta$  (A94V) suppresses the expressions of COX-2, GM-CSF, and CYP1A1 by blocking the nuclear translocation of NF- $\kappa$ B and AP-1, as well as inhibiting the activation of the AhR/ARNT signaling pathway. Our findings offer valuable insights into developing therapeutic strategies and potential drugs to mitigate PM-induced skin inflammation by inhibiting the ERK/p38/NF- $\kappa$ B/AP-1 and AhR/ARNT signaling pathways.

**Keywords** HaCaT, Fine dust, PM<sub>10</sub>, PAH, MAPK, Skin inflammation, one-point mutated IL-32 $\theta$  (A94V)

### Abbreviations

PM	Particulate matter
PM <sub>10</sub>	PM of 10 $\mu$ m or less
PAH	Polycyclic aromatic hydrocarbon
AD	Atopic dermatitis
AhRs	Aryl hydrocarbon receptors
ARNT	Aryl hydrocarbon nuclear translocator
ROS	Reactive oxygen species
IL	Interleukin
COX-2	Cyclooxygenase-2
GM-CSF	Granulocyte-macrophage colony stimulating factor
CYP	Cytochrome P450
qRT-PCR	Quantitative real-time reverse transcription polymerase chain reaction
ELISA	Enzyme-linked immunosorbent assay
MAPK	Mitogen-activated protein kinase
ERK	Extracellular signal-regulated kinase
JNK	c-Jun N-terminal kinase
NF- $\kappa$ B	Nuclear factor-kappa B
PBS	Phosphate-buffered saline

<sup>1</sup>Department of Bioscience and Biotechnology, Konkuk University, Seoul 05029, Republic of Korea. <sup>2</sup>Boson Bioscience, Cheongju 28161, Chungbuk, Republic of Korea. <sup>3</sup>College of Pharmacy & Medical Research Center, Chungbuk National University, Cheongju 28160, Republic of Korea. <sup>4</sup>Sookmyung Women's University, Seoul 04310, Republic of Korea. ✉email: yyang@sookmyung.ac.kr; ydy4218@konkuk.ac.kr

Increasing exposure to particulate matter (PM) in the air has become an issue threatening the quality of life, as polluted air constrains people's activities and lifestyles, negatively affects their health, and causes economic losses. PM also contributes to skin dysfunction and skin diseases<sup>1</sup>. Airborne PM smaller than 10  $\mu\text{m}$  ( $\text{PM}_{10}$ ) causes skin damage<sup>2</sup>. The skin is the first protective barrier in humans and is in direct contact with various air pollutants. PM contains volatile organic compounds, transition metals, carbonaceous materials, and polycyclic aromatic hydrocarbons (PAHs)<sup>3</sup>. Continuous exposure to environmental pollutants may cause skin damage, such as acne, psoriasis, and atopic dermatitis (AD)<sup>4</sup>. PAHs cause cellular oxidative damage to human keratinocytes by impairing redox homeostasis<sup>5</sup> and enhancing pro-inflammatory cytokines<sup>6</sup>. Human skin is composed of layers of epidermis, dermis, and hypodermis. The outermost layer of the epidermis is primarily composed of keratinocytes (95%). Keratinocytes are important cells in the epidermis as a physical barrier protecting the skin from pathogens, microbes, environmental toxicants, and harmful external stimuli, with a modulatory effect on skin immune responses<sup>7</sup>. Aryl hydrocarbon receptors (AhRs) play crucial roles in skin immunity and integrity as sensors for environmental chemicals and respond to exogenous and endogenous chemicals by regulating the expression of several genes essential for basic skin functions. The AhR signaling pathway is induced by small molecules such as environmental toxicants and bacterial pigments. Environmental toxicants such as PAHs may interact with the skin surface and be absorbed through the skin<sup>8</sup>. PAHs are toxic ligands of AhRs and ligand-activated transcription factors expressed in all skin cell types<sup>9</sup>. Activation of this receptor is known to upregulate several xenobiotics-metabolizing CYP enzymes, such as cytochrome p450s, particularly the isoforms 1A1 and 1B1 in keratinocytes<sup>10–12</sup>. CYP enzymes are responsible for the metabolism and detoxification of PAHs, producing activated PAHs. Activated PAHs and oxidized metabolites induce oxidative stress mediated via increasing reactive oxygen species (ROS)<sup>13</sup>. In particular, the enzymatic activity of CYP1A1 exacerbates ROS generation<sup>12</sup>. Oxidative stress via activation of the AhR-mediated pathway has been reported to relate to skin inflammation and skin diseases such as atopic dermatitis and psoriasis<sup>14</sup>. PAHs also induce the expression of cyclooxygenase-2 (COX-2) and pro-inflammatory cytokine granulocyte monocyte colony-stimulating factor (GM-CSF)<sup>15,16</sup>. PAHs activate the AhR and ERK/p38/AP-1/NF- $\kappa$ B signaling pathways, leading to COX-2 expression<sup>17</sup>. We also found that PAHs induce GM-CSF expression in human keratinocytes. GM-CSF drives the development of neutrophils, which play an essential role in the inflammation responses<sup>18</sup>. Increased levels of GM-CSF in inflamed tissues of AD patients may contribute to the chronicity of skin diseases<sup>19</sup>. Therefore, blocking AhR-mediated and ERK/p38/AP-1/NF- $\kappa$ B signaling pathways, could be attractive therapeutic targets for skin inflammation and skin diseases. Interleukin-32 (IL-32) is a cytokine expressed by human natural killer (NK) cells after stimulation by mitogen or IL-2<sup>20</sup>. IL-32 has been linked to cancer growth, chronic inflammatory disorders such as Crohn's disease, viral infections, inflammatory bowel disease, and rheumatoid arthritis, according to many studies. The IL-32 gene has eight exons with several splicing variants. IL-32 $\alpha$ , IL-32 $\beta$ , IL-32 $\gamma$ , and IL-32 $\delta$  were first discovered in NK cells, with IL-32 $\gamma$  having the longest sequence among the IL-32 isoforms<sup>20</sup>. IL-32 $\epsilon$ , IL-32 $\zeta$ , IL-32 $\eta$ , IL-32 $\theta$ , and IL32sm were additionally identified, and a total of nine isoforms have been reported<sup>21</sup>. Among them, IL-32 $\theta$  is the only isoform with no exon 6 except for IL-32sm. Recent research has demonstrated the anti-inflammatory and tumor-suppressive effects of wild type IL-32 $\theta$ <sup>22,23</sup>. Integrin  $\alpha\text{v}\beta 6$  is a part of the  $\alpha\text{v}$  integrin subfamily, which includes  $\alpha\text{v}\beta 1$ ,  $\alpha\text{v}\beta 3$ ,  $\alpha\text{v}\beta 5$ ,  $\alpha\text{v}\beta 6$ , and  $\alpha\text{v}\beta 8$ , and is found in the lungs, kidneys, and skin. This integrin is important for regulating inflammatory responses<sup>24</sup>. Additionally, integrin  $\alpha\text{v}\beta 6$  mediates inflammatory responses by activating two key signaling cascades: the extracellular signal-regulated kinase (ERK) pathway and the p38 MAPK pathway, both of which are essential regulators of inflammation<sup>25,26</sup>. A recent study demonstrated that integrin  $\alpha\text{v}$  inhibition decreased AhR activity and reduced AhR target gene CYP1A1 expression<sup>27</sup>. In a recent study, Park et al. revealed that this integrin could also act as a receptor for one-point mutated IL-32 $\theta$  (A94V)<sup>28</sup>. Although IL-32 $\theta$  (A94V) has shown therapeutic benefits, its effect on skin inflammation triggered by particulate matter (PMs) remains uncertain. In this study, we revealed for the first time that one-point mutated IL-32 $\theta$  (A94V) has an anti-inflammatory effect in  $\text{PM}_{10}$ -induced keratinocytes mediated via down-regulating  $\text{PM}_{10}$ -induced activation of ERK/p38/AP-1/NF- $\kappa$ B signaling pathways and inhibiting AhR activity. Our results demonstrated that IL-32 $\theta$  (A94V) down-regulated COX-2, GM-CSF, and CYP1A1 expressions mediated via AhR/ARNT and ERK/p38/AP-1/NF- $\kappa$ B signaling pathways.

## Results

### Identification of integrin $\alpha\text{v}\beta 6$ in HaCaT cells

We performed RT-PCR analysis to assess integrin subunits  $\alpha\text{v}$  and  $\beta 6$  expression in HaCaT cells, revealing that integrin subunits  $\alpha\text{v}$  and  $\beta 6$  were expressed in HaCaT keratinocytes (Fig. 1A). Similar to other  $\alpha$  and  $\beta$  isoforms of IL-32<sup>29</sup>, IL-32 $\theta$  (A94V) has recently been found to bind to the integrin  $\alpha\text{v}\beta 6$  known to play an important role in the modulation of the inflammatory responses<sup>24,28</sup>.

### IL-32 $\theta$ (A94V) inhibited COX-2 and GM-CSF gene and protein expressions in $\text{PM}_{10}$ -exposed HaCaT cells

To elucidate whether IL-32 $\theta$  (A94V) would modulate the expression of the inflammatory cytokines and mediators regulated via the integrin  $\alpha\text{v}\beta 6$ , which are expressed on the HaCaT keratinocytes (Fig. 1A), RT-qPCR and western blot analyses were performed to confirm whether IL-32 $\theta$  (A94V) would inhibit expressions of COX-2 and GM-CSF. Recent studies demonstrated the anti-inflammatory and tumor-suppressive effects of IL-32 $\theta$  in various cells<sup>22,23</sup>. As abnormal expressions of COX-2 and GM-CSF are critical events in skin inflammation, we investigated the effect of IL-32 $\theta$  (A94V) on  $\text{PM}_{10}$ -induced skin inflammation in HaCaT keratinocyte cells. To evaluate whether IL-32 $\theta$  (A94V) would inhibit expressions of COX-2 and GM-CSF in  $\text{PM}_{10}$ -exposed HaCaT cells, the cells were pre-treated with IL-32 $\theta$  (A94V) and then exposed to  $\text{PM}_{10}$ . qRT-PCR and western blot analyses showed that  $\text{PM}_{10}$  induced the mRNA and protein expression of COX-2 and GM-CSF in HaCaT cells

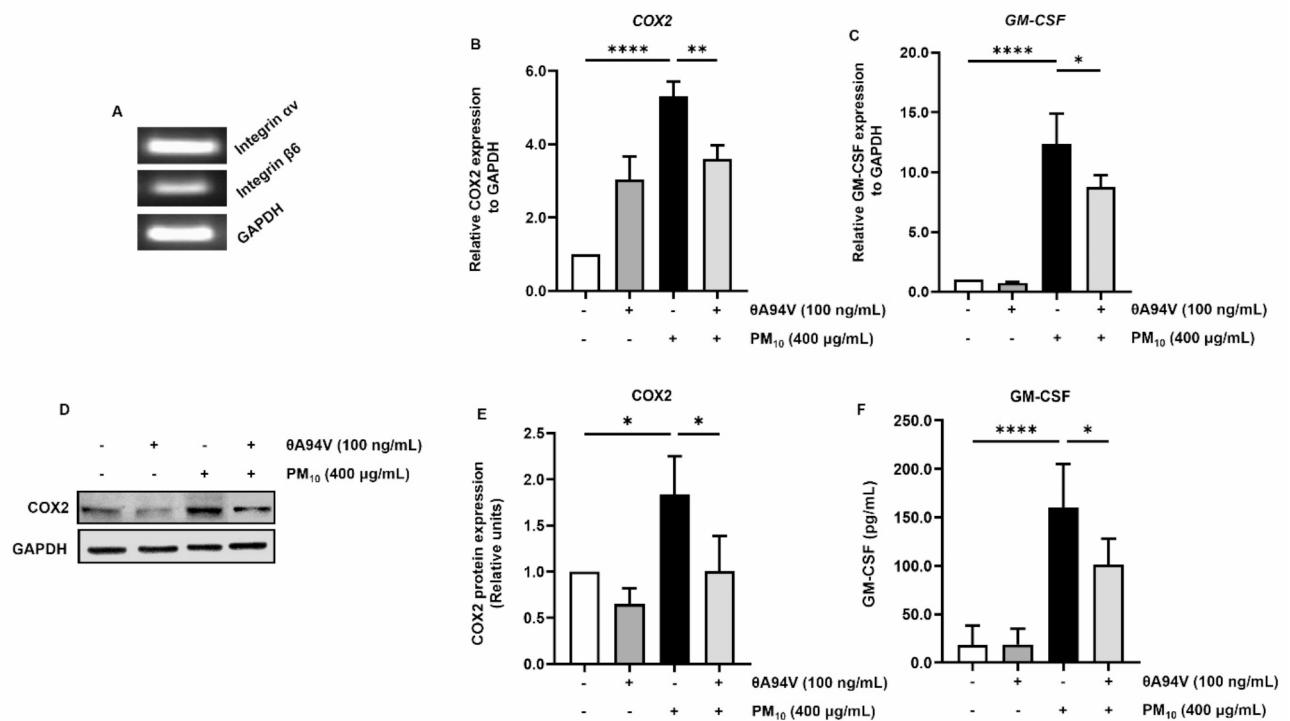


**Fig. 1.** Detection of integrin subunits  $\alpha v \beta 6$  expression in HaCaT cells and effects of IL-320 (A94V) on expression levels of COX-2 and GM-CSF in the PM<sub>10</sub>-exposed HaCaT cells. RT-PCR analysis was performed to assess integrin subunits  $\alpha v$  and  $\beta 6$  expression in HaCaT cells (A) as described in the Methods section. HaCaT cells were pre-treated with IL-320 (A94V) (100 ng/mL) for 1 h, and then treated with PM<sub>10</sub> (400  $\mu$ g/mL) for 24 h. mRNA levels of COX-2 and GM-CSF were evaluated by RT-qPCR (B and C), and protein levels of GM-CSF and COX-2 were evaluated by western blotting (D) and ELISA (F) and in the absence and presence of PM<sub>10</sub>. The band intensities of COX-2 were quantified using ImageJ software (E). GAPDH was used as the loading control. The data are presented as the means  $\pm$  SD ( $n = 3$ ).  $P$ -values were determined by one-way ANOVA. \* $p < 0.05$ , \*\* $p < 0.01$ , \*\*\*\* $p < 0.0001$ .

(Figs. 1B–F). Moreover, IL-320 (A94V) attenuated PM<sub>10</sub>-induced mRNA and protein expressions of COX-2 and GM-CSF (Fig. 1B–F). Please note that the original (full length and uncropped) blots of Fig. 1D are included in a Supplementary Information file (Supplementary Fig. S1).

### IL-320 (A94V) inhibited MAPKs phosphorylation in PM10-exposed HaCaT cells

The mitogen-activated protein kinases (MAPKs) pathway plays an important regulatory role in the production of proinflammatory cytokines and vital signal transduction in response to external stimuli that can lead to inflammatory diseases<sup>30</sup>. IL-320 (A94V) attenuated PM<sub>10</sub>-induced phosphorylation levels of extracellular signal-regulated kinases 1 and 2 (ERK 1/2) and p38 (Fig. 2). Please note that the original (full length and uncropped) blots of Fig. 3A are included in a Supplementary Information file (Supplementary Fig. S2 and Fig. S3). These results indicate that IL-320 (A94V) inhibits PM<sub>10</sub>-activated MAPK (ERK 1/2) and p38 resulting in down-regulation of COX-2 and GM-CSF (Fig. 1).

### IL-320 (A94V) inhibited activation of COX-2 and GM-CSF promoters in PM10-exposed HaCaT cells

To investigate the effects of IL-320 (A94V) on COX-2 promoter activity, transfection and dual-luciferase reporter assays were performed. HaCaT cells were transfected with luciferase plasmid vectors containing the COX-2 promoter for 24 h, pre-treated with IL-320 (A94V) at the indicated concentration for 1 h, followed by treatment with PM<sub>10</sub> (400  $\mu$ g/mL) for 3 h, followed by the luciferase assay. The result showed that IL-320 (A94V) down-regulated the promoter activity of COX-2 (Fig. 3A), confirming that IL-320 (A94V) inhibited the PM<sub>10</sub>-induced transcriptional activity of COX-2. Furthermore, ChIP was used to study the binding of NF- $\kappa$ B p50 and AP-1 c-Jun to the COX-2 and GM-CSF promoters. We designed primer pairs that could detect DNA fragments bound to p50 and c-Jun antibodies using NF- $\kappa$ B and AP-1 consensus regions on each promoter of COX-2 and GM-CSF (Fig. 3B)<sup>31–33</sup>. The digested chromatin bound to p50 and c-Jun antibodies was used to identify chromatin enrichment using RT-PCR and agarose gel electrophoresis. Primers for the ribosomal protein L30 (RPL30) gene were used as a positive control, as shown in lane 2 (Fig. 3C). Although the PCR products were found to increase in the positive control, IL-320 (A94V) attenuated the PM<sub>10</sub>-activated binding interactions of NF- $\kappa$ B p50 and AP-1 c-Jun into the COX-2 promoter (Fig. 3C and D); IL-320 (A94V) also diminished the PM<sub>10</sub>-

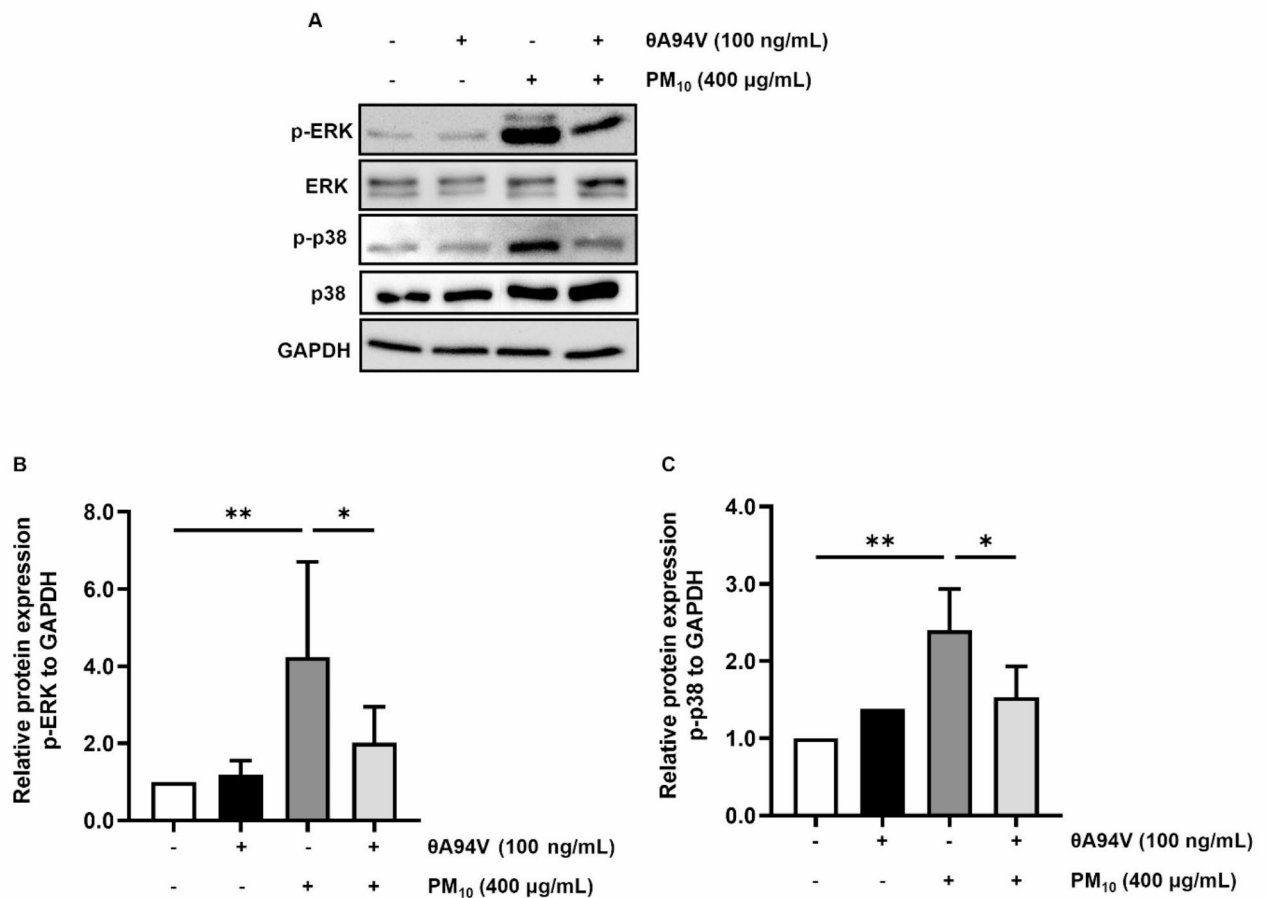


**Fig. 2.** Effects of IL-320 (A94V) on PM<sub>10</sub>-induced phosphorylation of MAPKs in HaCaT cells. HaCaT cells were pre-treated with IL-320 (A94V) (100 ng/mL) for 1 h, and then treated with PM<sub>10</sub> (400 µg/mL) for 24 h. The levels of phosphorylation of MAPKs were analyzed by western blot (A), and the band intensity was quantified using ImageJ software (B, C). GAPDH was used as the loading control. The data are presented as the means  $\pm$  SD ( $n = 3$ ). *P*-values were determined by one-way ANOVA. \* $p < 0.05$ , \*\* $p < 0.01$ .

induced binding of NF- $\kappa$ B (p50) to the GM-CSF promoter (Fig. 3C). These results indicated that IL-320 (A94V) could block the binding of the transcription factors (NF- $\kappa$ B p50 and AP-1 c-Jun) to the COX-2 promoter also inhibit the binding of NF- $\kappa$ B (p50) to the GM-CSF promoter in PM<sub>10</sub>-exposed HaCaT cells.

#### IL-320 (A94V) inhibited nuclear translocations of NF- $\kappa$ B and AP-1 in PM<sub>10</sub>-exposed HaCaT cells

I $\kappa$ B binds to NF- $\kappa$ B, forming an I $\kappa$ B: NF- $\kappa$ B complex, which can be disrupted in response to external stimuli. Upstream signals phosphorylate I $\kappa$ B, and once the complex is disrupted, NF- $\kappa$ B translocates to the nucleus<sup>34</sup>. Transcription factors such as NF- $\kappa$ B play key roles in regulating the transcription of target genes responsible for inflammatory responses<sup>35</sup>. To investigate the effect of IL-320 (A94V) on PM<sub>10</sub>-induced phosphorylation of I $\kappa$ B and the nuclear translocations of NF- $\kappa$ B and AP-1 in HaCaT cells, the cells were pre-treated with IL-320 (A94V) (100 ng/mL) for 1 h prior to exposure to PM<sub>10</sub> (400 µg/mL). We confirmed the phosphorylation level of I $\kappa$ B and nuclear translocation of NF- $\kappa$ B (p50) and AP-1 (c-Jun) using nuclear fractionation and western blotting. IL-320 (A94V) attenuated the PM<sub>10</sub>-induced I $\kappa$ B phosphorylation (Fig. 4A). In addition, as shown in Fig. 4B, PM<sub>10</sub>-induced nuclear translocations of p50 and c-Jun were found to be inhibited by IL-320 (A94V).

#### IL-320 (A94V) inhibited COX-2 and GM-CSF protein expressions by blockade of the NF- $\kappa$ B and AP-1 pathways in HaCaT cells

Western blotting and ELISA were performed to assess the involvement of NF- $\kappa$ B and AP-1 pathways in PM<sub>10</sub>-induced upregulations of COX-2 and GM-CSF in HaCaT cells. Treatment of HaCaT cells with PM<sub>10</sub> increased COX-2 and GM-CSF expression (Fig. 5). Similar to COX-2 and GM-CSF expression levels of NF- $\kappa$ B inhibitor Bay11-7082 or AP-1 inhibitor Tanshinone-treated cells, IL-320 (A94V) reduced COX-2 and GM-CSF expression levels (Fig. 5). Please note that the original (full length and uncropped) blots of Fig. 5A, B are included in a Supplementary Information file (Supplementary Fig. S4 and Fig. S5). These findings suggest that IL-320 (A94V) inhibits COX-2 and GM-CSF expressions mediated via NF- $\kappa$ B and AP-1 signaling pathways.

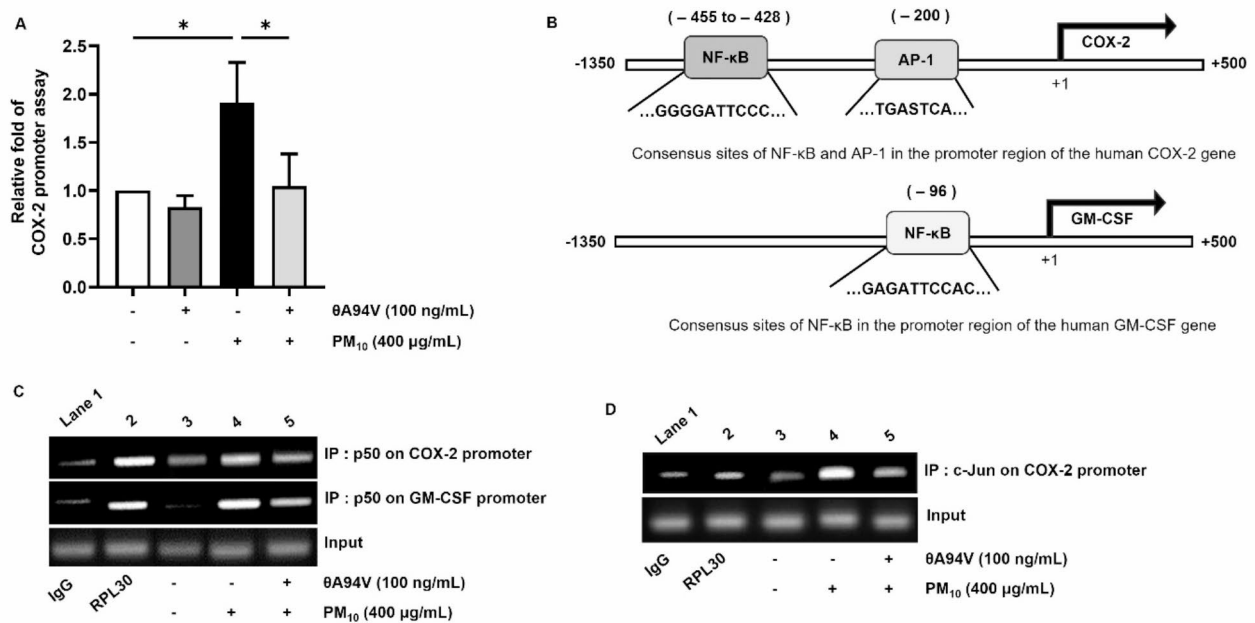


**Fig. 3.** Effects of IL-32θ (A94V) on COX-2 and GM-CSF promoter activities in the PM<sub>10</sub>-exposed HaCaT cells. The COX-2 promoter activity was analyzed by dual-luciferase reporter assay (A). HaCaT cells were transfected with COX-2 promoter for 24 h, then pre-treated with IL-32θ (A94V) (100 ng/mL) for 1 h, and then treated with PM<sub>10</sub> (400 µg/mL) for 24 h. DNA interactions of NF-κB and AP-1 were accessed by a chromatin immunoprecipitation (ChIP) assay. The consensus binding site sequences of COX-2 and GM-CSF are shown (B). RT-PCR analyses were performed to indicate the DNA interactions of NF-κB on COX-2 and GM-CSF promoters (C) and the DNA interaction of AP-1 (c-Jun) on COX-2 promoter (D). HaCaT cells were pre-treated with IL-32θ (A94V) (100 ng/mL) for 1 h and then treated with PM<sub>10</sub> (400 µg/mL) for 3 h. The data are presented as the means ± SD ( $n = 3$ ).  $P$ -values were determined by one-way ANOVA. \* $p < 0.05$  (A).

### IL-32θ (A94V) suppressed CYP1A1 expression in PM10-exposed HaCaT cells

Exposure to environmental toxicants such as polycyclic aromatic hydrocarbons (PAHs) exert their effects by binding to aryl hydrocarbon receptors (AhRs) and translocating them into the nucleus. After translocation, they form a complex with an aryl hydrocarbon nuclear translocator (ARNT). This complex binds to xenobiotic response elements (XREs), induces the expression of xenobiotic-metabolizing enzymes such as CYP1A1 and CYP1B1, affecting metabolism of heterogeneous substances that can induce ROS production and inflammation<sup>36</sup>. IL-32θ (A94V) suppressed CYP1A1 expression in PM<sub>10</sub>-exposed HaCaT cells (Fig. 6), supporting that IL-32θ (A94V) inhibits ROS production and inflammation response. Please note that the original (full length and uncropped) blots of Fig. 6C are included in a Supplementary Information file (Supplementary Fig. S6). Although IL-32θ (A94V) decreased CYP1A1 expression levels, it did not significantly affect CYP1B1 expression (data not shown).

### IL-32θ (A94V) inhibited expressions of COX-2 and GM-CSF by blockade of the AhR/ARNT pathway in HaCaT cells

AhR is a transcription factor that responds to endogenous and exogenous ligands, including environmental toxicants, such as PAHs and dioxins in PM. PM activates AhRs, causing them to translocate to the nucleus and bind to DNA elements<sup>11</sup>. Recent studies have suggested that AhRs are involved in oxidative stress and skin inflammation<sup>37</sup>. Western blotting revealed that PM<sub>10</sub> induces AhR/ARNT activation in the nucleus (Fig. 7A). Moreover, IL-32θ (A94V) significantly attenuated PM<sub>10</sub>-induced COX-2 and GM-CSF expressions similar to a selective AhR antagonist (CH223191) in HaCaT cells (Fig. 7B and C). Please note that the original (full length and uncropped) blots of Fig. 7B are included in a Supplementary Information file (Supplementary Fig. S7). These data indicated that COX-2 and GM-CSF expressions are up-regulated in response to PM<sub>10</sub> and suppressed by IL-32θ (A94V) via AhR signaling pathway.

### Discussion

Research on PM<sub>10</sub> effects has primarily focused on the respiratory, pulmonary, and cardiovascular diseases. Even though the skin is directly exposed to air pollutants, the extent of their harmful effects on the skin is still being investigated. Therefore, this study was focused on the association between exposure of PM<sub>10</sub> to skin inflammation. Air pollutants significantly affect inflammatory skin diseases by causing oxidative stress, triggering inflammation, and altering immune responses. In this study, we found that PM<sub>10</sub> increased the expression of COX-2 and GM-CSF in human keratinocyte HaCaT cells. Surprisingly, IL-32θ (A94V) demonstrated anti-inflammatory effects in PM<sub>10</sub>-exposed HaCaT cells. The role of COX-2 in the pathogenesis of skin disorders is crucial because agents



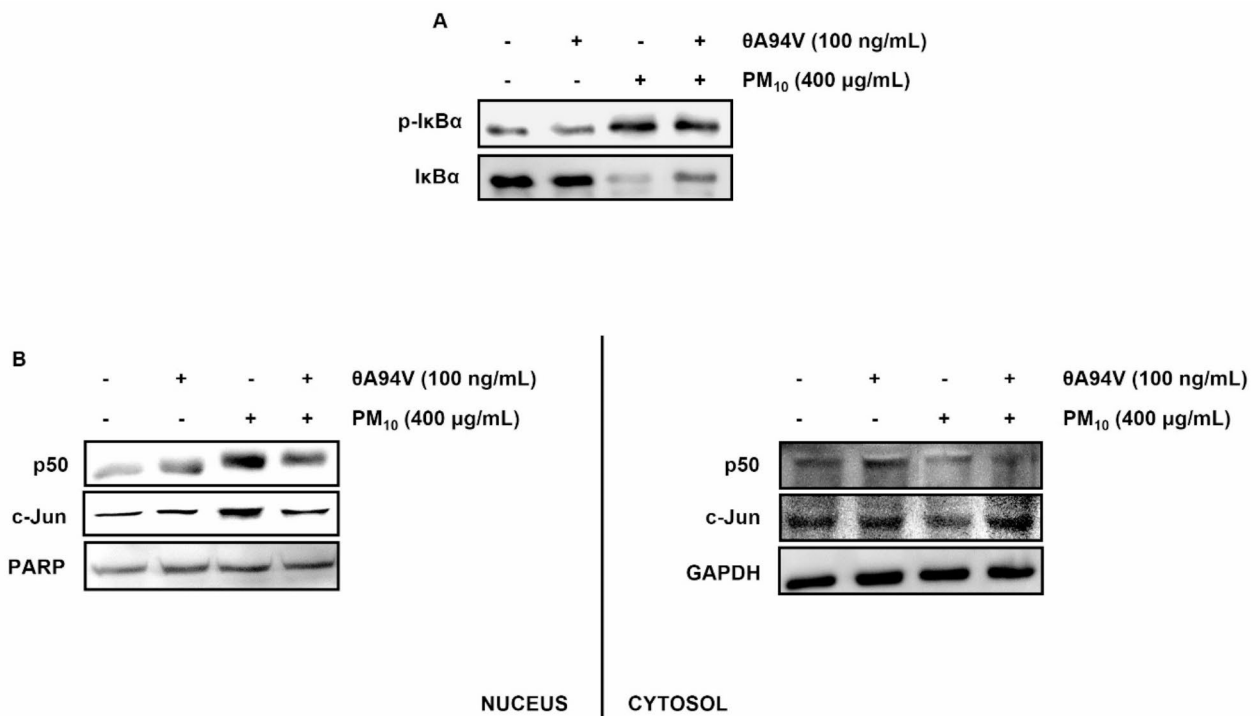


**Fig. 4.** Effects of IL-320 (A94V) on phosphorylation levels of IκB and nuclear translocation of NF-κB (p50) and AP-1 (c-Jun) in HaCaT cells. HaCaT cells were pre-treated with IL-320 (A94V) (100 ng/mL) for 1 h and then treated with PM<sub>10</sub> (400 μg/mL) for 3 h. The level of phosphorylation of IκB was analyzed by western blot (A). The nuclear p50 and c-Jun levels were determined by western blotting (B). Data represents one of three independent experiments.

targeting COX-2 are widely used for their anti-inflammatory effects as reported<sup>38</sup>. GM-CSF also plays a key role in various biological functions, such as mediating inflammation and pain, suggesting it can be a potential target for treating many inflammatory and autoimmune conditions<sup>39</sup>. The increased production of GM-CSF may contribute to the rise in eosinophils and the deposition of eosinophil granule proteins, which play a role in chronic allergic diseases such as atopic dermatitis (AD)<sup>19</sup>. Our RT-PCR analysis confirmed the expression of the integrin subunits αv and β6 in HaCaT keratinocytes (Fig. 1A). Interestingly, IL-320 (A94V) has recently been shown to bind to the integrin αvβ6, a key modulator of inflammatory responses<sup>24,28</sup>, similar to other IL-32α and β isoforms<sup>29</sup>. Furthermore, we demonstrated that IL-320 (A94V) significantly reduced the production of COX-2 and GM-CSF (Fig. 1B and D). PM<sub>10</sub>, such as PAHs, may cause inflammation by activating the MAPK signaling pathway<sup>40</sup>. Thus, our results suggest that the inhibitory effect of IL-320 (A94V) on the PM<sub>10</sub>-induced phosphorylation of ERK1/2 and p38 MAPKs (Fig. 2). The NF-κB and AP-1 signaling pathways are regulated by MAPKs and may be involved in regulating the production of COX-2 and GM-CSF. As shown in Fig. 4, IL-320 (A94V) inhibited PM<sub>10</sub>-induced IκB phosphorylation and the nuclear translocation of both NF-κB and AP-1 in HaCaT cells. Our experiments using NF-κB and AP-1 inhibitors confirmed that PM<sub>10</sub> induces the nuclear translocation of these transcription factors, highlighting their key role in the PM<sub>10</sub>-induced upregulation of inflammatory mediators COX-2 and GM-CSF. Moreover, IL-320 (A94V) attenuated these signaling pathways similarly to the effects of the AP-1 and NF-κB inhibitors (Fig. 5). We also performed a luciferase assay using COX-2 luciferase reporter plasmid to detect the activity of the COX-2 promoter in PM<sub>10</sub>-induced HaCaT cells and found that the activity of the COX-2 promoter induced by PM<sub>10</sub> was attenuated by IL-320 (A94V) (Fig. 3A). Additionally, ChIP assays revealed that IL-320 (A94V) attenuated binding activities of AP-1 (c-Jun) and NF-κB (p50) to the consensus binding sites on the COX-2 promoter, and NF-κB (p50) to the GM-CSF promoter in PM<sub>10</sub>-exposed HaCaT cells (Fig. 3B and D).

Additionally, it was reported that exposure to environmental toxicants found in PM, such as PAHs, activates AhR translocation from the cytosol to the nucleus and it forms a dimer with ARNT and upregulates CYP enzymes. PM-induced CYP enzymes, such as CYP1A1, metabolize PAHs to produce metabolites that can cause cell damage and generate reactive oxygen species (ROS) resulting in inflammation<sup>41</sup>. AhR functions as an important regulator of cellular homeostasis during inflammation, particularly in barrier organs, such as the skin and gut<sup>42</sup>. Recently, an increasing number of studies have highlighted the regulatory roles of AhR in skin physiology<sup>43</sup>. AhR is involved in triggering multiple inflammatory responses upon exposure to PM<sup>17</sup>. However, whether AhR inactivation can inhibit skin inflammation remains unclear. In the present study, we demonstrated that IL-320 (A94V) inhibited the AhR/ARNT signaling pathway and suppressed the expression of CYP1A1 (Figs. 6 and 7). Furthermore, to explore the role for AhR signaling in PM-induced upregulation of productions of COX-2 and GM-CSF, we utilized the AhR antagonist CH223191. Compared to PM<sub>10</sub> alone, treatment with

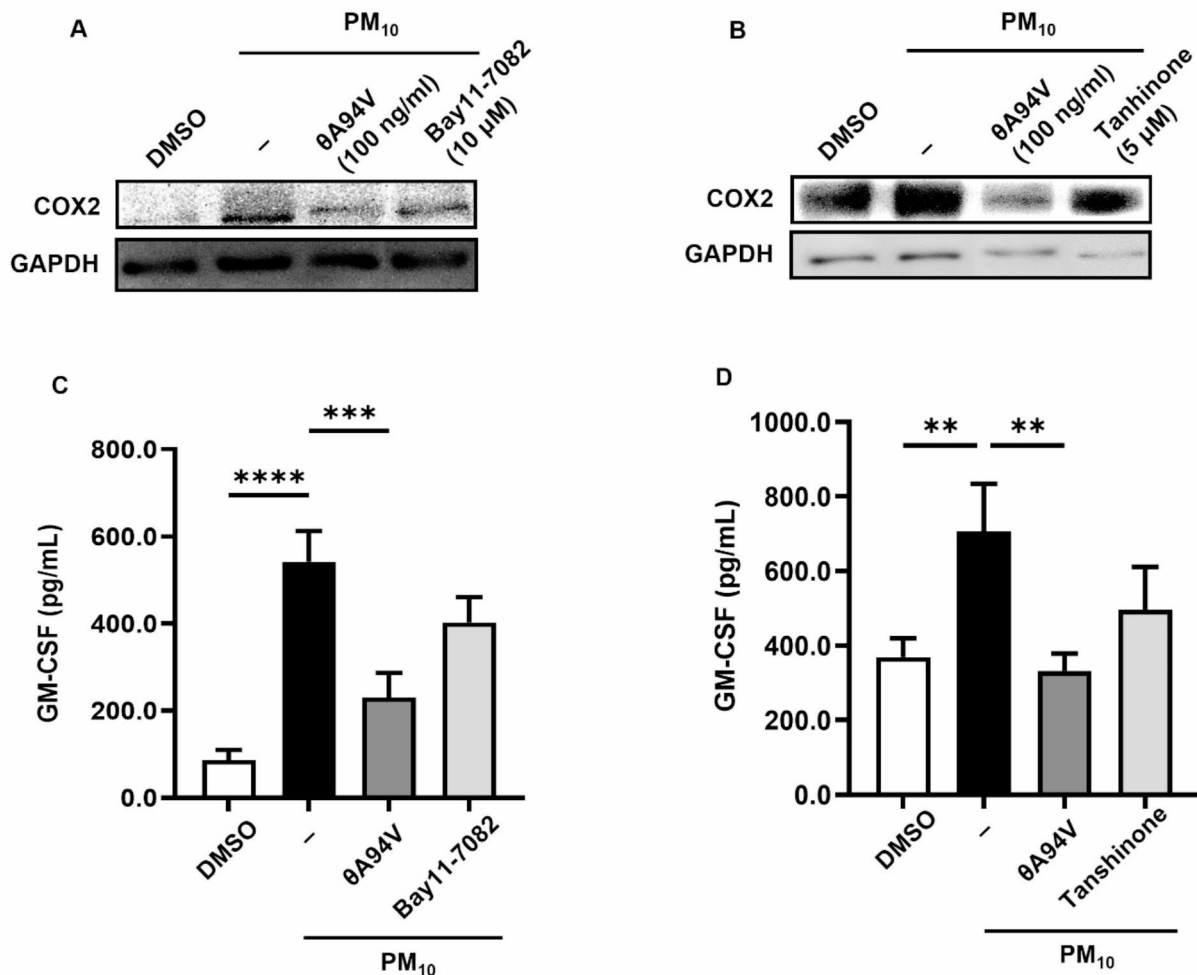


**Fig. 5.** Modulating effects of IL-32θ (A94V), NF-κB inhibitor, or AP-1 inhibitor on PM<sub>10</sub>-induced COX-2 and GM-CSF expression in HaCaT cells. HaCaT cells were treated with PM<sub>10</sub> (400 μg/mL) for 24 h in the presence or absence of NF-κB inhibitor Bay11-7082 (10 μM), AP-1 inhibitor Tanshinone (5 μM), or IL-32θ (A94V) (100 ng/mL). COX-2 protein level was analyzed by western blot (A). The secreted GM-CSF levels were determined by ELISA (B and C). The data are presented as the means ± SD (*n* = 3). *P*-values were determined by one-way ANOVA. \*\**p* < 0.01, \*\*\**p* < 0.001, \*\*\*\**p* < 0.0001.

IL-32θ (A94V) reduced PM<sub>10</sub>-induced expressions of COX-2 and GM-CSF in HaCaT cells, similar to the effects of the selective AhR antagonist (Fig. 7). Collectively, our findings reveal that PM<sub>10</sub> induces skin inflammation through multiple mechanisms, including enhanced COX-2 and GM-CSF production and increased CYP1A1 expression in human keratinocytes, leading to compromised skin barrier function. Importantly, we identified that the one-point mutated IL-32θ (A94V) demonstrates significant therapeutic potential by exerting anti-inflammatory effects through modulation of the ERK/p38/AP-1/NF-κB signaling pathways and the AhR/ARNT pathway (Fig. 8). These discoveries pave the way for developing innovative therapeutic approaches using IL-32θ (A94V) to address PM<sub>10</sub>-induced skin inflammation and associated conditions, potentially offering more effective strategies to maintain skin barrier function and reduce inflammation in humans.

While our use of human keratinocytes HaCaT cells provided valuable initial insights into skin immunological and inflammatory processes, the inclusion of multiple cell lines in future studies would broaden our understanding of these mechanisms. To bridge the gap between laboratory conditions and real-world scenarios, future investigations could explore varying PM concentrations and exposure durations. Building upon our encouraging *in vitro* findings, additional studies utilizing reconstructed human skin (RHS) models and diverse *in vivo* conditions would further validate our observations. Our results suggest that deeper investigation of these aspects could significantly advance the development of safer, more effective treatments for skin diseases.

## Conclusions

Our study shows that IL-32θ (A94V) mitigates skin inflammation caused by PM<sub>10</sub> exposure by suppressing the expression of COX-2, GM-CSF, and CYP1A1. This suppression occurs through the modulation of both ERK/p38/NF-κB and AP-1 signaling cascades, alongside the AhR/ARNT pathway in HaCaT human keratinocyte

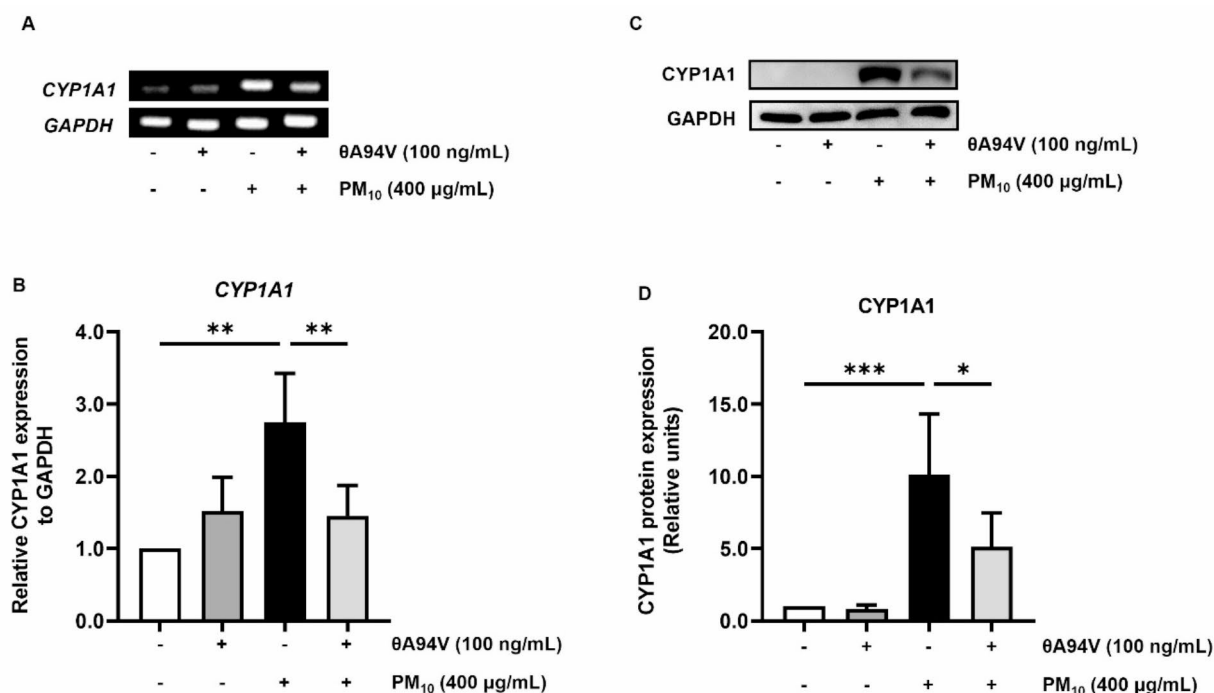


**Fig. 6.** Effects of IL-32θ (A94V) on mRNA and protein level of CYP1A1 in the PM<sub>10</sub>-exposed HaCaT cells. HaCaT cells were pre-treated with IL-32θ (A94V) (100 ng/mL) for 1 h and then treated with PM<sub>10</sub> (400 µg/mL) for 24 h. The mRNA level of CYP1A1 was analyzed by RT-PCR (A), and the band intensity was quantified using ImageJ software (B). The protein level of CYP1A1 was determined by western blotting (C), and the band intensity was quantified using ImageJ software (D). The data were presented as the means ± SD (*n* = 3). *P*-values were determined by one-way ANOVA. \**p* < 0.05, \*\**p* < 0.01, \*\*\**p* < 0.001.

cells. As the adverse effects of fine dust on human health become increasingly apparent, these insights offer promising directions for developing innovative treatments for PM<sub>10</sub>-related skin disorder.

## Methods

### Cell culture

The human skin keratinocyte HaCaT cells were obtained from Bogoo Biological Technology (Shanghai, China). The cells were cultured and maintained in Dulbecco's modified Eagle's medium (Welgene Incorporation, Daegu, Korea) supplemented with 10% fetal bovine serum (Hyclone Laboratories, Logan, UT, USA), penicillin (100 U/mL), and streptomycin (100 µg/mL). Cells were incubated in a 5% CO<sub>2</sub>-containing atmosphere at 37 °C and subjected to a maximum of 20 passages.

### Raw materials and reagents

ERM-certified FDP reference material ERM-CZ100 (PM<sub>10</sub>-like), an ingredient of PM<sub>10</sub>, was purchased from Merck (Darmstadt, Germany), suspended in phosphate-buffered saline (PBS), and homogenized by sonication for 60 min at room temperature to achieve a stock concentration of 50 mg/mL. IL-32θ (A94V) recombinant protein was purified as recently reported<sup>28</sup>.

### RNA extraction and RT-PCR

HaCaT cells (2 × 10<sup>5</sup> cells/well) were seeded into 6-well plates pre-treated with IL-32θ (A94V) for 1 h and then treated with PM<sub>10</sub> for 24 h. The treated cells were collected and lysed using the easy-BLUE™ Total RNA extraction kit (iNtRon Biotechnology, Seoul, South Korea) according to the manufacturer's instructions. For RT-PCR, RNA (1 µg) was reverse transcribed into cDNA using oligo (dT) primers and M-MuLV reverse transcriptase (New England Biolabs, Ipswich, MA, USA). The RNA was converted into cDNA using ProStar (Stratagene, La Jolla, CA, USA). The synthesized cDNA was amplified using a PCR Thermal Cycler Dice (Takara, Otsu, Shiga, Japan). The following sets of primers were used: Integrinαv: 5'-AGGAGAAGGTGCCTACGAAGCT (forward) and 5'-GCACAGGAAA GTCTTG CTAA GGC (reverse); Integrinβ6: 5'-TCTCTGCGTGAGACACAAAGG-3' (forward) and 5'-GAGCACTCCATCTTCAGAGACG-3' (reverse); glyceraldehyde-3-phosphate dehydrogenase (GAPDH): 5'-TGA TGA CAT CAA GAA GGT (forward) and 5'-TCC TTG GAG GCC ATG TAG GCC (reverse). GAPDH was used as an internal control. The PCR products were separated on a 2% agarose gel.



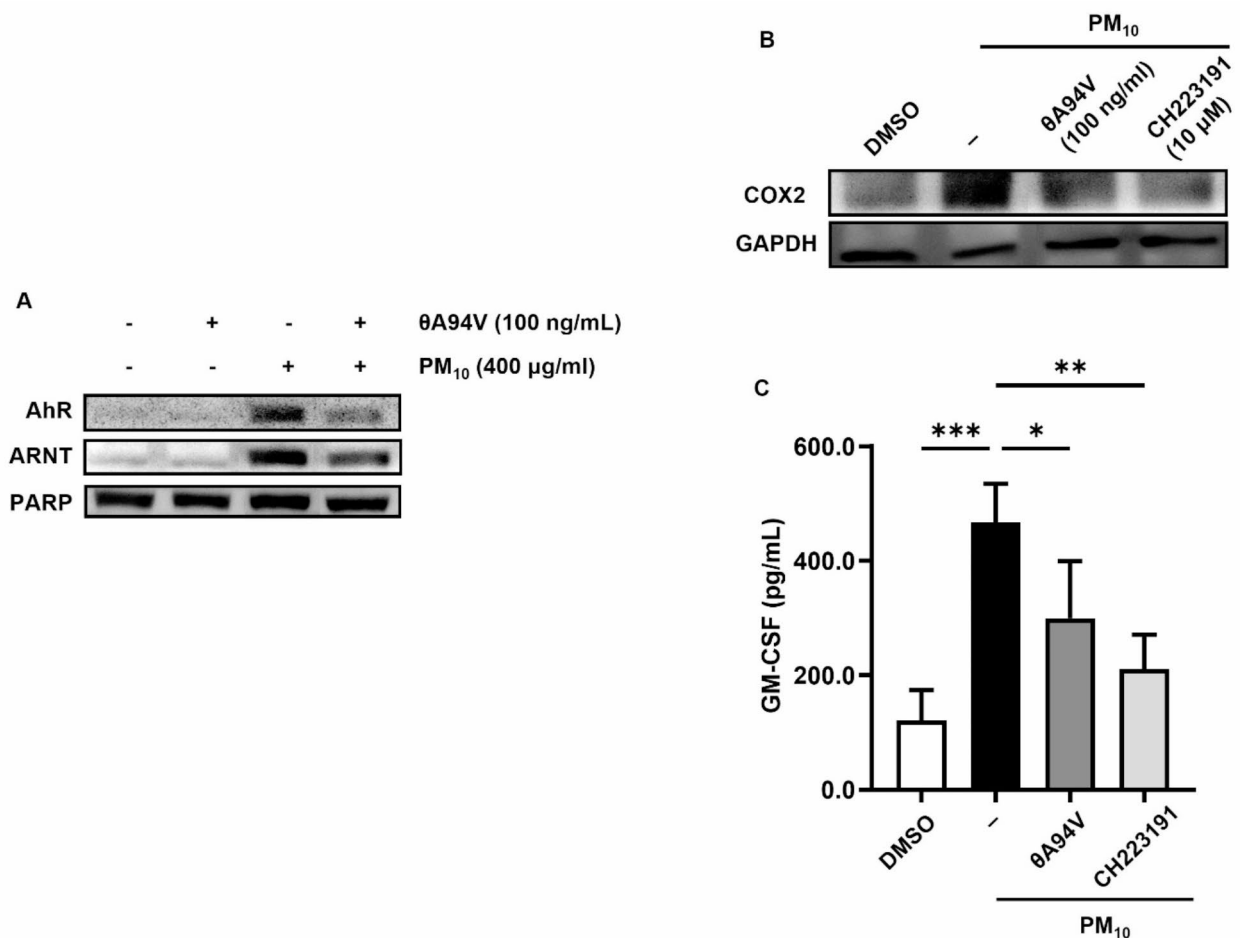


**Fig. 7.** Effects of IL-32θ (A94V) on PM<sub>10</sub>-induced activation of AhR/ARNT in HaCaT cells. HaCaT cells were pre-treated with IL-32θ (A94V) (100 ng/mL) for 1 h and then treated with PM<sub>10</sub> (400 µg/mL) for 3 h. Representative western blotting of AhR protein in the nucleus after pre-treatment with IL-32θ (A94V) in the presence or absence of PM<sub>10</sub> (A). To assess whether AhR inactivation can inhibit skin inflammation, HaCaT cells were pre-treated with AhR antagonist CH223191 before PM<sub>10</sub> treatment. The protein levels of COX-2 and GM-CSF were determined by western blotting and ELISA (B and C). The data were presented as the means ± SD (*n* = 3). *P*-values were determined by one-way ANOVA. \**p* < 0.05, \*\**p* < 0.01, \*\*\**p* < 0.001 (C).

#### qRT-PCR

The IL-32θ (A94V)-treated cells were harvested, and RNA was extracted using an easy-BLUE™ Total RNA extraction kit (iNtRon Biotechnology) according to the manufacturer's instructions. The cDNA products were obtained using M-MuLV reverse transcriptase (New England Biolabs, Beverly, MA, USA). RT-PCR was performed with a relative quantification protocol using Rotor-Gene 6000 series software 1.7 (Qiagen, Hilden, Germany) and Sensi FAST™ SYBR NO-ROX Kit (BIOLINE, London, UK). The expression of all target genes was normalized to that of the housekeeping gene GAPDH. Each sample was run with the following primer sets: COX-2: 5'-CGG TGA AAC TCT GGC TAG ACA G -3' (forward) and 5'-GCA AAC CGT AGA TGC TCA GGG A-3' (reverse); GM-CSF: 5'-AAA TGT TTG ACC TCC AGG AG-3' (forward) and 5'-TGA TAA TCT GGG TTG CAC AG-3' (reverse); GAPDH: 5'-TGA TGA CAT CAA GAA GGT (forward) and 5'-TCC TTG GAG GCC ATG TAG GCC (reverse). GAPDH was used as an internal control.

#### ELISA

HaCaT cells ( $3 \times 10^5$  cells/well) were plated in 6-well plates for 24 h and pre-treated with IL-32θ (A94V) or the AhR antagonist CH223191, NF-κB inhibitor Bay11-7082, or AP-1 inhibitor Tanshinone for 1 h prior to treatment with PM<sub>10</sub> (400 µg/mL), respectively. The protein levels of GM-CSF in the cell culture media were determined by ELISA (R&D Systems, Minneapolis, MN, USA). A flat-bottom 96-well plate was coated with mouse monoclonal anti-human GM-CSF at 2 µg/mL in PBS. After blocking with bovine serum albumin (BSA) in PBS, 100 µL of the sample was added to each well. Subsequently, the wells were incubated for 2 h at room temperature with 100 µL of biotinylated goat anti-human GM-CSF at 10 ng/mL (1% BSA in PBS), followed by incubation with streptavidin-conjugated horseradish peroxidase in PBS containing 0.1% BSA and 0.05% Tween-20. The color developed after the addition of tetramethylbenzidine, and the reaction was stopped by

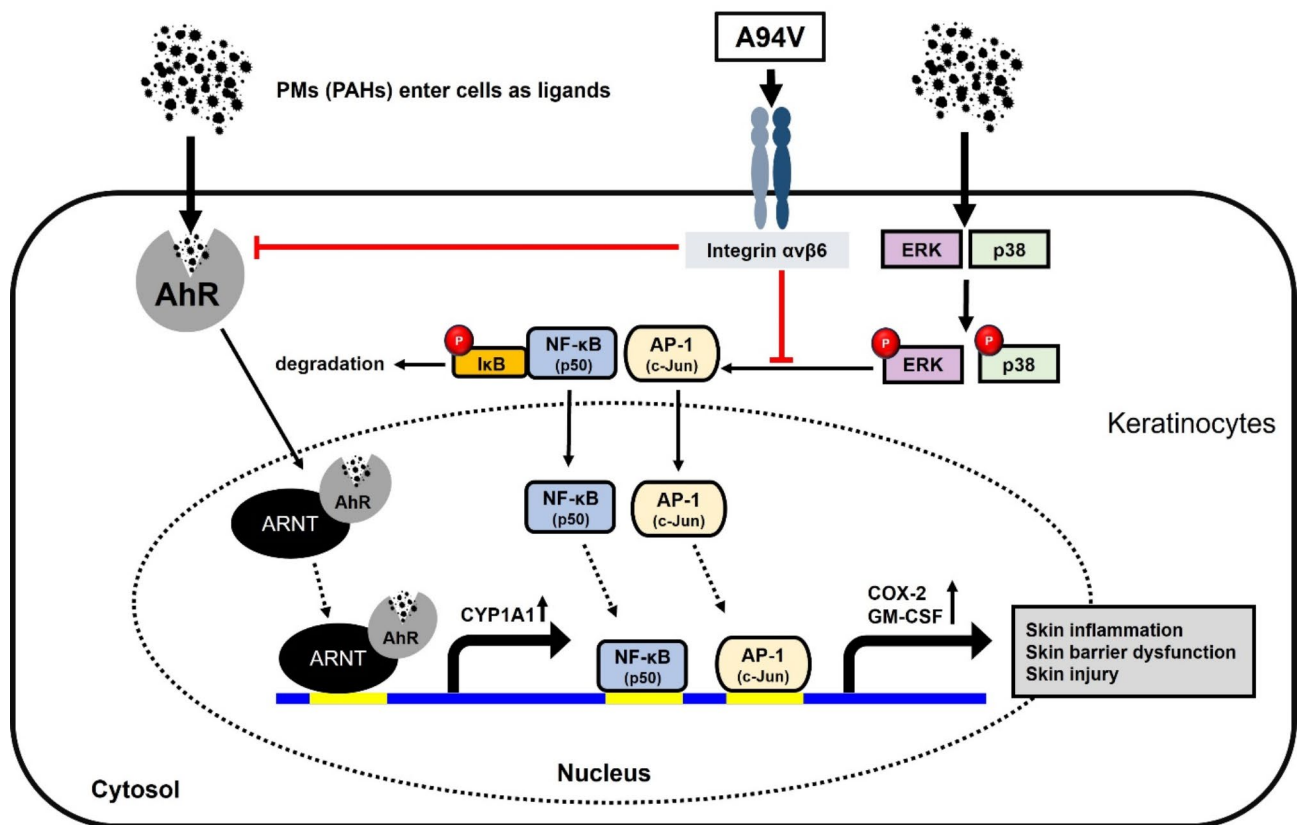


**Fig. 8.** Schematic overview of the proposed inhibitory signaling pathway of IL-320 (A94V) on the production of COX-2, GM-CSF, and CYP1A1, mediated by targeting AhR and integrin for the treatment of skin inflammatory diseases. Upon binding to ligands such as PMs (PAHs), AhRs translocate to the nucleus and bind to ARNT. This complex then attaches to XREs on DNA, upregulating the expression of COX-2, GM-CSF, and CYP1A1. Additionally, PMs (PAHs) induce the expressions of COX-2 and GM-CSF by stimulating the ERK/p38/ NF-κB/AP-1 pathways in HaCaT cells. IL-320 (A94V) inhibits the expression of COX-2, GM-CSF and CYP1A1 by targeting both the AhR/ARNT pathway and the ERK/p38/NF-κB/AP-1 pathways mediated through integrin signaling.

adding 2.5 N  $\text{H}_2\text{SO}_4$  solution. The color was quantified using an Apollo LB 9110 microplate reader at 450 nm (corrected by absorption at 570 nm).

#### Nuclear and cytoplasmic fractionation

HaCaT cells were pre-treated with IL-320 (A94V) (100 ng/mL) for 1 h, and then treated with  $\text{PM}_{10}$  (400  $\mu\text{g}/\text{mL}$ ) for 3 h before fractionation using NE-PER nuclear and cytoplasmic extraction reagents (Thermo Fisher Scientific Inc., Waltham, MA, USA) according to the manufacturer's instructions. Equal quantities of protein from these extracts (50  $\mu\text{g}$ ) were separated by sodium dodecyl sulfate-polyacrylamide gel electrophoresis and transferred to polyvinylidene difluoride membranes. The subsequent steps for the procedure were followed as described for western blotting. Primary antibodies against p50 and c-Jun were used in the nuclear fractions. PARP was used as a nuclear protein marker.

#### Western blotting

HaCaT cells ( $4 \times 10^5$  cells/well) were plated in 6-well plates for 24 h and pre-treated for 1 h with IL-320 (A94V) (100 ng/mL) followed by treatment with  $\text{PM}_{10}$  (400  $\mu\text{g}/\text{mL}$ ) for 24 h. The cells were lysed in a buffer containing 50 mM Tris (pH 7.4), 150 mM NaCl, 1% NP-40, 0.1% sodium dodecyl sulfate (SDS), 0.25% sodium deoxycholate, 1 mM ethylenediaminetetraacetic acid, 1 mM ethylene glycol tetraacetic acid, 1 mM orthovanadate, aprotinin (10  $\mu\text{g}/\text{mL}$ ), and 0.4 mM phenylmethylsulfonyl fluoride at 4 °C for 2 h. The cells were lysed, and the protein content was estimated using the Bradford assay reagent (Bio-Rad Laboratories, Hercules, CA, USA) and a UV spectrophotometer, as previously reported<sup>44</sup>. Proteins (30  $\mu\text{g}$ ) were separated on 10% sodium dodecyl sulfate-polyacrylamide gels and transferred onto polyvinylidene fluoride membranes. Membranes were blocked with 5% skimmed milk for 1 h at room temperature and incubated with primary antibodies against MAPKs, including phospho-ERK (Cell Signaling Technology, Danvers, MA, USA, Cat#9101S), ERK (Santa Cruz Biotechnology, Dallas, Texas, Cat#sc-94), phospho-p38 (Cell Signaling Technology, Cat#9211S), p38 (Cell Signaling Technology, Cat#8690S), COX-2 (Santa Cruz Biotechnology, Cat#sc-376861), CYP1A1 (ABclonal, Woburn, MA, USA, Cat#A22182), AhR (Santa Cruz Biotechnology, Cat#sc-133088), ARNT (ABclonal, Cat#A19532), PARP (Cell

Signaling Technology, Cat#9542S), and GAPDH (Santa Cruz Biotechnology, Cat#sc-47724) for 1 h at room temperature. After incubation, the membranes were incubated with the mouse-IgGκ light chain binding protein conjugated to horseradish peroxidase (HRP) (m-IgGκ BP-HRP) or goat anti-rabbit IgG-heavy and light chain antibody conjugated to HRP for 1 h at room temperature. Finally, the protein bands were visualized using an enhanced chemiluminescence western blotting detection kit (WesternBright™ ECL, Advansta, CA, USA). Densitometric graphs from three independent experiments were generated using ImageJ software version 1.5. The band intensities were normalized to those of GAPDH.

### Luciferase assay

The pGL3-luciferase reporter plasmid containing COX-2 was constructed as previously described<sup>45</sup>. In brief, the targeted COX-2 promoter region (-486 to +106 bp) was amplified by PCR from THP-1 genomic DNA. 5'-CGG GGT ACC AAG ACG TAC AGA CCA GAC AC-3' (forward) and 5'-GGA AGA TCT GGT AGG CTT TGC TGT CTG AG-3' (reverse). The PCR product was digested with *KpnI* and *BglII* restriction enzymes, and the digested fragment was ligated into the pGL3 basic vector, as previously described<sup>45</sup>. Then, the pGL3-COX-2 promoter construct (1 µg) was transfected into the cells using Lipofectamine 2000 (Invitrogen, Carlsbad, CA, USA), as previously reported. The transfected cells were pre-treated with IL-320 (A94V) for 1 h and treated with PM<sub>10</sub> (400 µg/mL) for 3 h. Luciferase assays were performed using a Dual-Luciferase Reporter Assay System (Promega, Madison, WI, USA). Firefly luciferase activity was measured using VICTOR X3 (PerkinElmer Inc., Waltham, MA, USA) and normalized to Renilla luciferase activity.

### Chromatin immunoprecipitation assay

Following the manufacturer's instructions, a chromatin immunoprecipitation (ChIP) assay was performed using a Simple ChIP Enzymatic Chromatin IP kit (Cell Signaling Technology). HaCaT cells (2 × 10<sup>6</sup> cells/well) were pre-treated with IL-320 (A94V) for 1 hour and then exposed to PM<sub>10</sub> for 3 hours and cross-linked with 1% (vol/vol) formaldehyde (Sigma) for 10 minutes at room temperature. Glycine was added to stop cross-linking, and the cells were washed with PBS three times. The cells were lysed with buffer A/B, and the chromatin was digested with micrococcal nuclease for 20 min at 37°C. Chromatin digestion was stopped by adding 0.5 M EDTA, and the nuclei were sonicated three times with 20-sec pulses at 30 to break the nuclear membrane. The cross-linked chromatin was incubated with 1 µg of anti-p50 (Cell Signaling Technology) and anti-c-Jun (Cell Signaling Technology) overnight at 4°C with rotation. Histone H3 monoclonal antibody and normal rabbit IgG were used as the positive and negative controls, respectively. After incubation with 30 µL of ChIP-grade protein G agarose beads for 2 hours at 4°C, the cross-links were reversed and eluted from the beads and digested with proteinase K for 2 hours at 65°C. After the reversal of the crosslinks, the DNA was purified using a spin column and amplified by RT-PCR. PCR was performed using the following primers that amplify the binding site of NF-κB in the COX-2 promoter: 5'-TCTAA AGACGTACAGACCAGACAC-3' (forward) 5'-GTTTCCGCCAGATG TCTTTTCTT-3' (reverse), AP-1 in the COX-2 promoter: 5'-CAC CGG GCT TAC GCA ATT TT-3' (forward) 5'-ACG CTC ACT GCA AGT CGT AT-3' (reverse), NF-κB in the GM-CSF promoter: 5'-TTG TTC AGC TGT TCT GTT CA-3' (forward) 5'-TTGGTGTCCAAGACAATGCA-3' (reverse). As controls, we used PCR primers for detection of the ribosomal protein L30 (RPL30) gene according to the manufacturer's instructions.

### Statistical analysis

Data are presented as mean ± SD. GraphPad Prism 5 (GraphPad Software Inc., San Diego, CA, USA) was used for the statistical analysis. One-way analysis of variance (ANOVA) followed by Tukey's honest significant difference test was performed. Statistical significance was set at  $p < 0.05$ .

### Data availability

All data supporting the findings from this study are available from the corresponding author upon reasonable request.

Received: 10 September 2024; Accepted: 11 December 2024

Published online: 15 January 2025

### References

1. Fernando, I. P. S. et al. Effects of (-)-Lololide against fine dust preconditioned keratinocyte media-induced dermal fibroblast inflammation. *Antioxidants* **10**(5) <https://doi.org/10.3390/antiox10050675> (2021).
2. Magnani, N. D. et al. Skin damage mechanisms related to airborne particulate matter exposure. *Toxicol. Sci.* **149**(1), 227–236 <https://doi.org/10.1093/toxsci/kfv230> (2016).
3. Kermani, M. et al. Extraction and determination of organic/inorganic pollutants in the ambient air of two cities located in metropolis of Tehran. *Environ. Monit. Assess.* **194**(3), 204 <https://doi.org/10.1007/s10661-021-09705-8> (2022).
4. Ferrara, F., Prieux, R., Woodby, B. & Valacchi, G. Inflammation activation in pollution-induced skin conditions. *Plast. Reconstr. Surg.* **147**(1S-2), 15S-24S <https://doi.org/10.1097/PRS.00000000000007617> (2021).
5. Soeur, J. et al. Photo-pollution stress in skin: Traces of pollutants (PAH and particulate matter) impair redox homeostasis in keratinocytes exposed to UVA1. *J. Dermatol. Sci.* **86**(2), 162–169 <https://doi.org/10.1016/j.jdermsci.2017.01.007> (2017).
6. Choi, H. & Kim, C. S. Polycyclic aromatic hydrocarbons from fine particulate matter induce oxidative stress and the inflammatory response in human vocal fold fibroblast cells. *Oxid. Med. Cell. Longev.* **2021**, 5530390 <https://doi.org/10.1155/2021/5530390> (2021).
7. Lawton, S. Anatomy and function of the skin, part 1. *Nurs. Times*. **102**, 3126–3127 (2006).
8. VanRooij, J. G., De Roos, J. H., Bodelier-Bade, M. M. & Jongeneelen, F. J. Absorption of polycyclic aromatic hydrocarbons through human skin: differences between anatomical sites and individuals. *J. Toxicol. Environ. Health*. **38**(4), 355–368 <https://doi.org/10.1080/15287399309531724> (1993).

9. Napolitano, M. & Patruno, C. Aryl hydrocarbon receptor (AhR) a possible target for the treatment of skin disease. *Med. Hypotheses*. **116**, 96–100 <https://doi.org/10.1016/j.mehy.2018.05.001> (2018).
10. Merk, H. F. Aryl hydrocarbon receptor signalling in the skin and adverse vemurafenib effects. *J. Eur. Acad. Dermatol. Venereol.* **32**(8), 1233–1234 <https://doi.org/10.1111/jdv.15148> (2018).
11. O'Driscoll, C. A. & Mezrich, J. D. The aryl hydrocarbon receptor as an immune-modulator of atmospheric particulate matter-mediated autoimmunity. *Front. Immunol.* **9**, 2833 <https://doi.org/10.3389/fimmu.2018.02833> (2018).
12. Fernandez-Gallego, N., Sanchez-Madrid, F. & Cibrián, D. Role of AHR ligands in skin homeostasis and cutaneous inflammation. *Cells* **10**(11) <https://doi.org/10.3390/cells10113176> (2021).
13. Rao, P. S. & Kumar, S. Polycyclic aromatic hydrocarbons and cytochrome P450 in HIV pathogenesis. *Front. Microbiol.* **6**, 550 <https://doi.org/10.3389/fmicb.2015.00550> (2015).
14. Kim, H. B. et al. Aryl hydrocarbon receptors: evidence of therapeutic targets in chronic inflammatory skin diseases. *Biomedicines* **10**(5) <https://doi.org/10.3390/biomedicines10051087> (2022).
15. Ferecatu, I. et al. Polycyclic aromatic hydrocarbon components contribute to the mitochondria-antiapoptotic effect of fine particulate matter on human bronchial epithelial cells via the aryl hydrocarbon receptor. *Part. Fibre Toxicol.* **7**, 18 <https://doi.org/10.1186/1743-8977-7-18> (2010).
16. Tanaka, M. et al. Polycyclic aromatic hydrocarbons in urban particle matter exacerbate movement disorder after ischemic stroke via potentiation of neuroinflammation. *Part. Fibre Toxicol.* **20**(1), 6 <https://doi.org/10.1186/s12989-023-00517-x> (2023).
17. Lee, C. W. et al. Urban particulate matter down-regulates filaggrin via COX2 expression/PGE2 production leading to skin barrier dysfunction. *Sci. Rep.* **6**, 27995 <https://doi.org/10.1038/srep27995> (2016).
18. Hamilton, J. A. GM-CSF in inflammation. *J. Exp. Med.* **217**(1) <https://doi.org/10.1084/jem.20190945> (2020).
19. Bratton, D. L. et al. Granulocyte macrophage colony-stimulating factor contributes to enhanced monocyte survival in chronic atopic dermatitis. *J. Clin. Invest.* **95**(1), 211–218 <https://doi.org/10.1172/JCI117642> (1995).
20. Kim, S. H., Han, S. Y., Azam, T., Yoon, D. Y. & Dinarello, C. A. Interleukin-32: a cytokine and inducer of TNF $\alpha$ . *Immunity* **22**(1), 131–142 <https://doi.org/10.1016/j.immuni.2004.12.003> (2005).
21. Kang, J. W. et al. Interaction network mapping among IL-32 isoforms. *Biochimie* **101**, 248–251 <https://doi.org/10.1016/j.biochi.2014.01.013> (2014).
22. Bak, Y. et al. IL-32 $\theta$  downregulates CCL5 expression through its interaction with PKC $\delta$  and STAT3. *Cell. Signal.* **26**(12), 3007–3015 <https://doi.org/10.1016/j.cellsig.2014.09.015> (2014).
23. Pham, T. H. et al. Interleukin-32 $\theta$  inhibits tumor-promoting effects of macrophage-secreted CCL18 in breast cancer. *Cell. Commun. Signal.* **17**(1), 53 <https://doi.org/10.1186/s12964-019-0374-y> (2019).
24. Song, Y. et al. Role of integrin  $\alpha$ v $\beta$ 6 in acute lung injury induced by *Pseudomonas aeruginosa*. *Infect. Immun.* **76**(6), 2325–2332 <https://doi.org/10.1128/IAI.01431-07> (2008).
25. Yan, P. et al. Integrin  $\alpha$ v $\beta$ 6 promotes lung cancer proliferation and metastasis through upregulation of IL-8-mediated MAPK/ERK signaling. *Transl. Oncol.* **11**(3), 619–627 <https://doi.org/10.1016/j.tranon.2018.02.013> (2018).
26. Xue, B. et al. Stromal cell-derived factor-1 (SDF-1) enhances cells invasion by  $\alpha$ v $\beta$ 6 integrin-mediated signaling in ovarian cancer. *Mol. Cell. Biochem.* **380** (1–2), 177–184 <https://doi.org/10.1007/s11010-013-1671-1> (2013).
27. Silgner, M. et al. The aryl hydrocarbon receptor links integrin signaling to the TGF- $\beta$  pathway. *Oncogene* **35**(25), 3260–3271 <https://doi.org/10.1038/nc.2015.387> (2016).
28. Park, J. Y. et al. Human IL-32 $\theta$ A94V mutant attenuates monocyte-endothelial adhesion by suppressing the expression of ICAM-1 and VCAM-1 via binding to cell surface receptor integrin  $\alpha$ V $\beta$ 3 and  $\alpha$ V $\beta$ 6 in TNF- $\alpha$ -stimulated HUVECs. *Front. Immunol.* **14**, 1160301 <https://doi.org/10.3389/fimmu.2023.1160301> (2023).
29. Heinhuis, B. et al. Interleukin 32 (IL-32) contains a typical  $\alpha$ -helix bundle structure that resembles focal adhesion targeting region of focal adhesion kinase-1. *J. Biol. Chem.* **287**(8), 5733–5743 <https://doi.org/10.1074/jbc.M111.288290> (2012).
30. Huang, P., Han, J. & Hui, L. MAPK signaling in inflammation-associated cancer development. *Protein Cell.* **1**(3), 218–226 <https://doi.org/10.1007/s13238-010-0019-9> (2010).
31. Schmedtje, J. F. Jr., Ji, Y. S., Liu, W. L., DuBois, R. N. & Runge, M. S. Hypoxia induces cyclooxygenase-2 via the NF- $\kappa$ B p65 transcription factor in human vascular endothelial cells. *J. Biol. Chem.* **272**(1), 601–608 <https://doi.org/10.1074/jbc.272.1.601> (1997).
32. Yang, C. C., Hsiao, L. D., Shih, Y. F., Su, M. H. & Yang, C. M. Sphingosine 1-phosphate-upregulated COX-2/PGE(2) system contributes to human cardiac fibroblast apoptosis: involvement of MMP-9-dependent transactivation of EGFR cascade. *Oxid. Med. Cell. Longev.* **2022**, 7664290 <https://doi.org/10.1155/2022/7664290> (2022).
33. McCaffrey, P. G., Jain, J., Jamieson, C., Sen, R. & Rao, A. A T cell nuclear factor resembling NF-AT binds to an NF- $\kappa$ B site and to the conserved lymphokine promoter sequence cytokine-1. *J. Biol. Chem.* **267**(3), 1864–1871 (1992).
34. Karin, M. How NF- $\kappa$ B is activated: the role of the IkappaB kinase (IKK) complex. *Oncogene* **18**(49), 6867–6874 <https://doi.org/10.1038/sj.onc.1203219> (1999).
35. Rummel, C. Inflammatory transcription factors as activation markers and functional readouts in immune-to-brain communication. *Brain Behav. Immun.* **54**, 1–14 <https://doi.org/10.1016/j.bbi.2015.09.003> (2016).
36. Sun, Y. et al. Benzo(a)pyrene induces MUC5AC expression through the AhR/mitochondrial ROS/ERK pathway in airway epithelial cells. *Ecotoxicol. Environ. Saf.* **210**, 111857 <https://doi.org/10.1016/j.ecoenv.2020.111857> (2021).
37. Dec, M. & Arasiewicz, H. Aryl hydrocarbon receptor role in chronic inflammatory skin diseases: a narrative review. *Postepy Dermatol. Alergol.* **41**(1), 9–19 <https://doi.org/10.5114/ada.2023.135617> (2024).
38. Lee, J. L., Mukhtar, H., Bickers, D. R., Kopelovich, L. & Athar, M. Cyclooxygenases in the skin: pharmacological and toxicological implications. *Toxicol. Appl. Pharmacol.* **192**(3), 294–306 [https://doi.org/10.1016/s0041-008x\(03\)00301-6](https://doi.org/10.1016/s0041-008x(03)00301-6) (2003).
39. Achuthan, A. A., Lee, K. M. C. & Hamilton, J. A. Targeting GM-CSF in inflammatory and autoimmune disorders. *Semin Immunol.* **54**, 101523 <https://doi.org/10.1016/j.smim.2021.101523> (2021).
40. Wang, J. et al. Urban particulate matter triggers lung inflammation via the ROS-MAPK-NF- $\kappa$ B signaling pathway. *J. Thorac. Dis.* **9**(11), 4398–4412 <https://doi.org/10.21037/jtd.2017.09.135> (2017).
41. Dijkhoff, I. M. et al. Impact of airborne particulate matter on skin: a systematic review from epidemiology to in vitro studies. *Part. Fibre Toxicol.* **17**(1), 35 <https://doi.org/10.1186/s12989-020-00366-y> (2020).
42. Kyoreva, M. et al. CYP1A1 enzymatic activity influences skin inflammation via regulation of the AHR pathway. *J. Invest. Dermatol.* **141**(6), 1553–63.e3 <https://doi.org/10.1016/j.jid.2020.11.024> (2021).
43. Napolitano, M. et al. Role of aryl hydrocarbon receptor activation in inflammatory chronic skin diseases. *Cells* **10**(12) <https://doi.org/10.3390/cells10123559> (2021).
44. Bradford, M. M. A rapid and sensitive method for the quantitation of microgram quantities of protein utilizing the principle of protein-dye binding. *Anal. Biochem.* **72**, 248–254 <https://doi.org/10.1006/abio.1976.9999> (1976).
45. Kim, S. J. et al. (E)-2-Methoxy-4-(3-(4-methoxyphenyl) prop-1-en-1-yl) phenol attenuates PMA-induced inflammatory responses in human monocytic cells through PKC $\delta$ /JNK/AP-1 pathways. *Eur. J. Pharmacol.* **825**, 19–27 <https://doi.org/10.1016/j.ejphar.2018.01.024> (2018).

## Acknowledgements

We would like to thank Editage ([www.editage.co.kr](http://www.editage.co.kr)) for their assistance with English language editing (no.

KOUNI-5704).

### Author contributions

Jinju Kim: methodology, validation, formal analysis, writing of the original draft, visualization, and editing. Chae-Min Lim: Methodology and investigation. Nahyun Kim: methodology and investigation. Hong-Gyum Kim: methodology and investigation. Jin-Tae Hong: methodology and formal analysis. Young Yang: conceptualization, methodology, formal analysis, writing original draft and review, editing, supervision, and funding acquisition. Do-Young Yoon: conceptualization, methodology, formal analysis, writing of the original draft and review, editing, supervision, and funding acquisition.

### Funding

This research was supported by the National Research Foundation of Korea (NRF), South Korea (NRF-2021R1A2C3003414, NRF-2021R1A6A1A03038890, and RS-2024-00451912).

### Declarations

### Competing interests

The authors declare no competing interests.

### Additional information

**Supplementary Information** The online version contains supplementary material available at <https://doi.org/10.1038/s41598-024-83159-z>.

**Correspondence** and requests for materials should be addressed to Y.Y. or D.-Y.Y.

**Reprints and permissions information** is available at [www.nature.com/reprints](http://www.nature.com/reprints).

**Publisher's note** Springer Nature remains neutral with regard to jurisdictional claims in published maps and institutional affiliations.

**Open Access** This article is licensed under a Creative Commons Attribution-NonCommercial-NoDerivatives 4.0 International License, which permits any non-commercial use, sharing, distribution and reproduction in any medium or format, as long as you give appropriate credit to the original author(s) and the source, provide a link to the Creative Commons licence, and indicate if you modified the licensed material. You do not have permission under this licence to share adapted material derived from this article or parts of it. The images or other third party material in this article are included in the article's Creative Commons licence, unless indicated otherwise in a credit line to the material. If material is not included in the article's Creative Commons licence and your intended use is not permitted by statutory regulation or exceeds the permitted use, you will need to obtain permission directly from the copyright holder. To view a copy of this licence, visit <http://creativecommons.org/licenses/by-nc-nd/4.0/>.

© The Author(s) 2024, corrected publication 2025